Polymer 50 (2009) 1228–1235

Contents lists available at ScienceDirect

Polymer

journal homepage: www.elsevier.com/locate/polymer

Interfacial behavior of high performance organic fibers

A. Andres Leal [a,b], Joseph M. Deitzel [a], Steven H. McKnight [d], John W. Gillespie, Jr. [a,b,c,*]

[a] Center for Composite Materials (UD-CCM), University of Delaware, Newark, DE 19716, United States
[b] Department of Materials Science and Engineering, University of Delaware, Newark, DE 19716, United States
[c] Department of Civil and Environmental Engineering, University of Delaware, Newark, DE 19716, United States
[d] Army Research Laboratory, Materials Division, Aberdeen, MD 21005, United States

ARTICLE INFO

Article history:
Received 6 June 2008
Received in revised form
23 December 2008
Accepted 10 January 2009
Available online 15 January 2009

Keywords:
Organic fiber
Interfacial shear strength
Polymer composite materials

ABSTRACT

The surface and interfacial properties of different high performance fibers of current interest have been analyzed. The pyridobisimidazole fiber M5 shows a markedly higher polar contribution to its surface free energy than the rest of the organic fibers under study. Interfacial shear strength (IFSS) values measured by means of the microdroplet test indicate that M5 fiber has an IFSS that doubles that of the Kevlar fibers, in agreement with the observed results from surface free energy tests. Armos fiber, a para-aramid material that incorporates imidazole functional groups, shows an average IFSS 30–35% higher than the Kevlar fibers. SEM micrographs of failed microdroplet specimens show different failure mechanisms for the Kevlar KM2, Armos and M5 fibers. The KM2 specimens fail due to complete detachment of surface fibrils from the bulk of the fiber, while Armos specimens fail by the combined effect of microfibrillation on the fiber surface coupled with adhesive failure. In contrast, M5 microdroplet specimens exhibit failure surfaces consisting of partial matrix yielding during droplet debonding, indicative of the high level of interfacial bonding to the surface and higher levels of hydrogen bonding within the fiber that suppress microfibrillation. The higher polar character of the M5 surface can lead to the presence of an interphase region with different mechanical properties from the bulk matrix.

1. Introduction

The use of organic fibers as reinforcing elements for composite materials in weight-sensitive, high performance applications is a viable alternative that stems from the high specific tensile strength and energy absorption capabilities shown by these fibers. Among the organic fibers of current interest, emerging materials such as M5 and Armos are particularly attractive, with tensile properties that exceed those of conventional high performance fibers such as Kevlar and E-glass [1]. In addition, M5 fiber also shows compressive properties that are higher than any other organic fiber has shown before [2]. As the mechanical properties of emerging organic fibers equal or surpass the properties of traditional reinforcing fibers, their use as reinforcements for composite materials needs to be evaluated in terms of their interactions with polymer matrices. In the case of composites for impact performance, weak fiber–resin interactions and high sliding friction are desirable to enhance their energy absorption capabilities. Structural applications, on the other hand, demand strong interactions in order to achieve load transfer between fiber and matrix. Fiber–resin interactions such as the degree of chemical bonding and physical interlocking are governed by the wetting behavior of the fiber. Intimate contact between solid and liquid is a necessary condition for good adhesion, which in turn, plays an important role for long-term durability of the composite. The chemical structure of M5 and Armos differs from traditional aramid materials commonly used as reinforcing elements. This makes the study of fiber–resin interactions a necessary step in order to tailor an interface to meet specific needs and applications.

Aramid fibers, the high performance organic fibrous material most widely used in varying commercial and industrial applications, offer a relatively smooth and inert surface, which limits potential chemical and/or mechanical interactions with polymeric resin systems, precluding the formation of an interphase region with characteristics that differ from fiber and resin. Numerous efforts have been made in order to enhance the interfacial interactions between aramid and other organic fibers and different resin systems. One of the most popular approaches in the literature has been the use of plasma and laser treatments that modify the chemical and morphological characteristics of fiber surfaces. The use of oxygen plasma treatments has resulted in an improvement of the polar component of the surface free energy of aramid fibers in the

* Corresponding author. Center for Composite Materials (UD-CCM), University of Delaware, Newark, DE 19716, United States. Tel.: +1 302 831 8149; fax: +1 302 831 8525.
E-mail address: gillespi@udel.edu (J.W. Gillespie Jr.).

0032-3861/$ – see front matter © 2009 Elsevier Ltd. All rights reserved.
doi:10.1016/j.polymer.2009.01.018

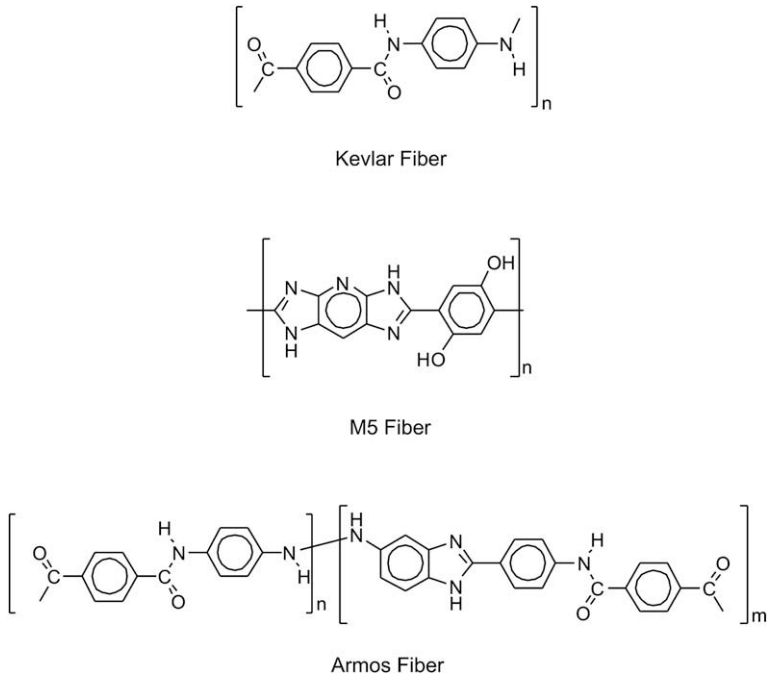

Fig. 1. Chemical structures of high performance organic fibers under study [11,12].

order of 30% [3,4]. Aramid fiber polar surface free energy improvements induced by oxygen plasma treatment have been shown by Park et al. to be directly proportional to improvements in the measured interfacial shear strength of this fiber [5]. In contrast to the mostly chemically based interfacial property improvements achieved by oxygen plasma treatment of aramid fibers, laser ablation of aramid fibers induces surface micro-corrugations that lead to a 120% improvement of the interfacial shear strength of aramid fiber [6].

The different micro-mechanical techniques available for the measurement of single fiber interfacial properties have been described in detail by Herrera Franco and Drzal. These include the microdroplet, fiber push-out, fiber fragmentation and fiber pull-out tests [7]. Andrews et al. have shown that the use of in situ Raman spectroscopy in conjunction with the micro-mechanical techniques listed above results in a precise mapping of stress and strain distribution as a function of applied load [8]. In the case of aramid fibers, different authors have pointed to the inadequacy of the fiber fragmentation test due to the high tensile failure strain and fibrillar fracture associated with most aramid fibers [7–9]. The fibrillar structure of high performance organic fibers makes the fiber push-out and micro-indentation techniques unsuitable to measure their interfacial properties [7–9], while the small diameter ($\sim$12 μm) of high performance organic fibers is described as a major drawback for the use of the fiber pull-out technique [9,10].

The present work analyzes the surface properties of different high performance organic fibers. Model composites are used to determine the interfacial behavior of the fibers by means of the microdroplet test, allowing one to identify the effect of the observed fiber surface properties on their interfacial performance. The role of fiber internal shear strength on the failure mode of the model composites is clearly illustrated.

2. Experimental

2.1. Materials

The high performance organic fibers included in the analysis are the pyridobisimidazole fiber M5®, the phenylene terephthalamide (aramid) fibers Kevlar® 49 and Kevlar® KM2, and the para-aramid Armos® fiber. The chemical structures of these fibers are shown in Fig. 1 [11,12].

M5 fibers, produced by Magellan Systems International LLC, were provided by the US Army Natick Research, Development and Engineering Center, the Armos Neutral (Armos N, pH 6.5) and Armos Acid (Armos A, pH 3.5) fibers were obtained from Tver'Khimvolokno Open Joint Stock Company, and the Kevlar 49 and Kevlar KM2 fibers were obtained from E. I. du Pont de Nemours and Company.

2.2. Dynamic contact angle measurements

Dynamic contact angle experiments were performed using a Cahn DCA-322 Dynamic Contact Angle Analyzer. Motor calibration and balance calibration were performed prior to testing. A set speed of 12 μm/s with advance and recede motions of 3 mm was used with all fiber specimens. The specimens were stored in a desiccator for 24 h prior to testing. The test liquids used and their corresponding surface free energies (γ) are listed in Table 1.

Fibers were tested as received. For each type of fiber, tests were performed with the 3 different test liquids reported in Table 1. For each liquid, 5–6 specimens were tested. After testing each specimen, the contact angle experimental values were obtained using the WinDCA software.

2.3. Microdroplet test

The microdroplet test, also referred to as the microbond test, is a micro-mechanical pull-out technique that applies a measured

Table 1
Surface free energy of test liquids [13].

Test liquid	γ^d (dynes/cm)	γ^p (dynes/cm)	γ^{total} (dynes/cm)
HPLC water	22.0	50.2	72.2
Glycerol	34.0	30.0	64.0
Hexadecane	27.6	0.0	27.6

force on a solid matrix droplet located on the free end of a single filament until fiber–matrix interfacial failure is achieved. Specimen preparation for the microdroplet test consists of applying a droplet of uncured resin in the liquid state, approximately 100–120 μm in diameter, to a single fiber, followed by curing and post-curing of the applied resin droplet. An optical micrograph of a microdroplet specimen is shown in Fig. 2. D.E.R.® 353 epoxy resin from The Dow Chemical Company was used with Amicure® PACM 20 curing agent from Air Products, mixed in a ratio of 100 parts of epoxy resin and 28 parts of curing agent. The resin used, a modified bisphenol-A/F based resin, is a low viscosity epoxy with an enhanced crystallization resistance that facilitates the formation of uniform, symmetric droplets on the single fibers. The applied resin droplets were cured for 2 h at 80 °C, followed by a post-curing cycle of 2 h at 150 °C.

Once the solid resin droplet has been post-cured, the specimen is mounted on the microdroplet testing machine, illustrated in Fig. 3. The knives come in contact with the solid resin droplet and the force required to debond the droplet from the fiber is recorded. The interfacial shear strength (IFSS) is calculated as a function of force to debond (F), fiber diameter (d), and droplet length (L):

$$\text{IFSS} = \frac{F}{\pi * d * L} \tag{1}$$

3. Results and discussion

3.1. Surface properties

Dynamic contact angles have been measured for the different organic filaments using the Wilhelmy plate and microbalance technique. The KM2 and Armos fibers have proprietary sizings to prevent property degradation from water adsorption, while the M5 material has not been sized. Water-sized E-glass filaments were also tested for a baseline comparison. Fig. 4 shows the advancing contact angle for each fiber in HPLC grade water, glycerol, and hexadecane. A contact angle (θ) of zero indicates that spontaneous spreading occurs, while $0^\circ < \theta < 90^\circ$ is indicative of attractive interactions, and $\theta > 90^\circ$ signifies repulsive interactions.

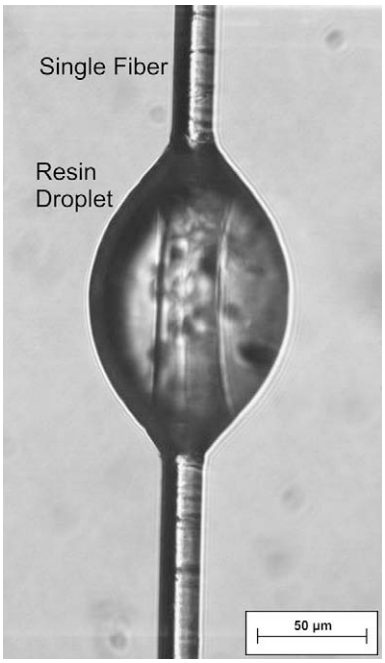

Fig. 2. Microdroplet test specimen.

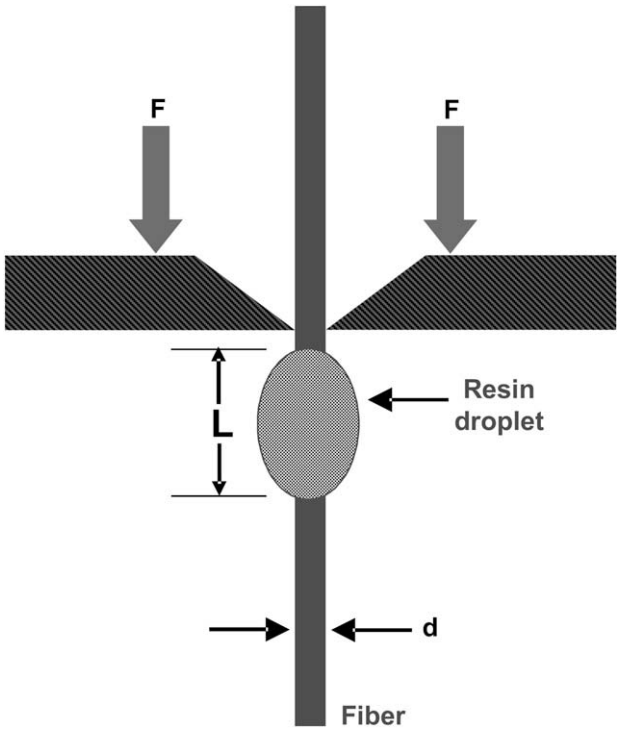

Fig. 3. Microdroplet test geometry.

From Fig. 4, the water-sized E-glass fiber has the lowest contact angles for the HPLC water and glycerol standard liquids, while the organic fibers show comparable wetting properties for these two standard liquids. In the case of hexadecane, a standard liquid that has no polar contribution to its surface free energy, the water-sized E-glass fiber also has one of the lowest contact angles (17°), although in this case the value is comparable to the contact angles measured for the Armos and Kevlar KM2 fibers, while the contact angle obtained for the M5 fiber is much larger (42°).

The polar (γ_s^p) and dispersive (γ_s^d) components of the fiber surface energy are determined from the measured fiber contact angle values (θ) in each of the solvents. The contact angle values and the known surface free energy of the solvents are used to plot the best-fit line using Equation (2) [13].

$$\frac{\gamma_{lv}(1+\cos\theta)}{2\sqrt{\gamma_{lv}^d}} = \left(\frac{\sqrt{\gamma_{lv}^p}}{\sqrt{\gamma_{lv}^d}}\right)\sqrt{\gamma_s^p} + \sqrt{\gamma_s^d} \tag{2}$$

where γ is the surface free energy. The superscripts p and d refer to the polar and dispersive contributions to the surface free energy of a given material and the subscripts s and lv refer to the fiber and liquid–vapor surfaces, respectively. The slope and intercept of the best-fit line from Equation (2) give $(\gamma_s^p)^{1/2}$ and $(\gamma_s^d)^{1/2}$, respectively, and the surface free energy of the fiber is then given by [13]:

$$\text{Total Surface Energy} = \gamma_s^p + \gamma_s^d \tag{3}$$

Fig. 5 shows the resulting surface energies for the tested fibers. The surface free energy is a measure of intermolecular forces due to the difference in energy between molecules at the surface and molecules in the bulk material. It allows one to determine parameters such as adsorption, adhesion, and wetting, as well as the nature and extent of the interphase region. The dispersion (London) contribution of the surface energy is due to electron motion, while the polar (Keesom) contribution is due to permanent dipole moments.

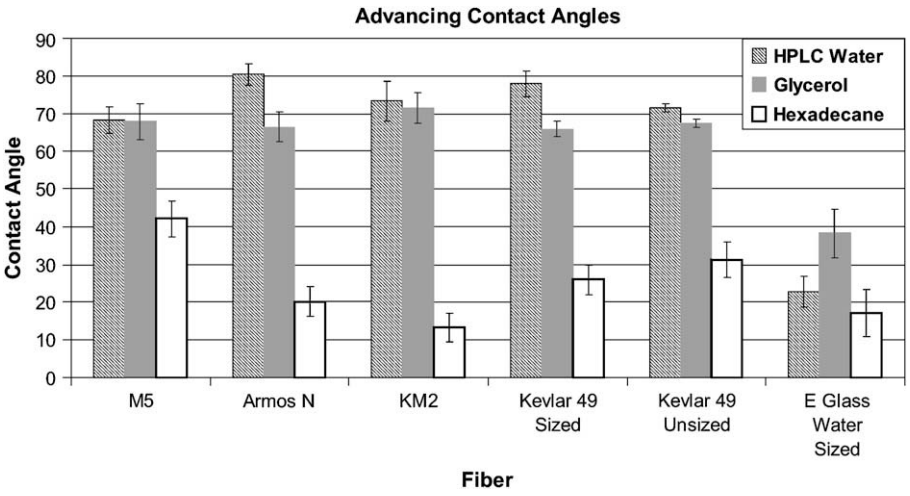

Fig. 4. Advancing contact angles of high performance fibers in different standard liquids.

The total surface free energy of the tested fibers provides an indication of the degree of wetting. The work of spreading, defined as the change in free energy required to spread the liquid over one unit area of solid, is directly proportional to the total surface free energy. For spontaneous spreading to occur (the energy of the two surfaces in contact is less than the energy of the two surfaces apart) the work of spreading must be greater than or equal to zero. In general, high-energy surfaces will wet better than low-energy surfaces for a given liquid. The water-sized E-glass fiber has the highest total surface free energy from all the tested fibers. As a result of the application of water to the fiber immediately after manufacture, the water-sized E-glass has a very polar, hydroxylated surface, which gives this fiber a much higher polar contribution of surface free energy than the rest of the tested fibers, and the highest total surface free energy. The measured surface free energy of water-sized E-glass fiber is in good agreement with values reported by Larson and Drzal [14].

The organic fibers show similar values of total surface free energy. However, M5 fiber does have a higher polar contribution than the rest of the organic fibers. The polar character of the M5 surface may cause the segregation of low molecular weight polar components of a resin, such as amines, at the fiber/matrix interface, in a manner similar to that seen in carbon fiber composites [15]. This segregation can lead to an interphase region at the fiber surface whose mechanical properties are different from the bulk matrix [15]. Additionally, the presence of the pendent hydroxyl groups could provide a means for commercially available silane based sizing to attach to the surface of the M5 fiber.

3.2. Interfacial properties

The interfacial shear strength (IFSS) between the fibers and an epoxy resin has been analyzed by means of the microdroplet test. In order to have a successful microdroplet test, the fiber–droplet interface should fail before fiber tensile failure takes place. Since the force needed to debond the droplet is directly proportional to the droplet size (L) (Fig. 3), it is important to determine the range of droplet sizes that will produce successful tests prior to specimen preparation. The cumulative probability of fiber tensile failure during microdroplet testing as a function of droplet size (L) can be calculated, for a given IFSS value, by means of the tensile strength values previously used to calculate the cumulative probability of failure from single fiber tensile testing [1]. The force needed to fail each specimen in tension is obtained from the tensile strength value (σ) of the specimen. The relationship between fiber tensile strength (σ), droplet size (L) and IFSS is expressed in Equation (4):

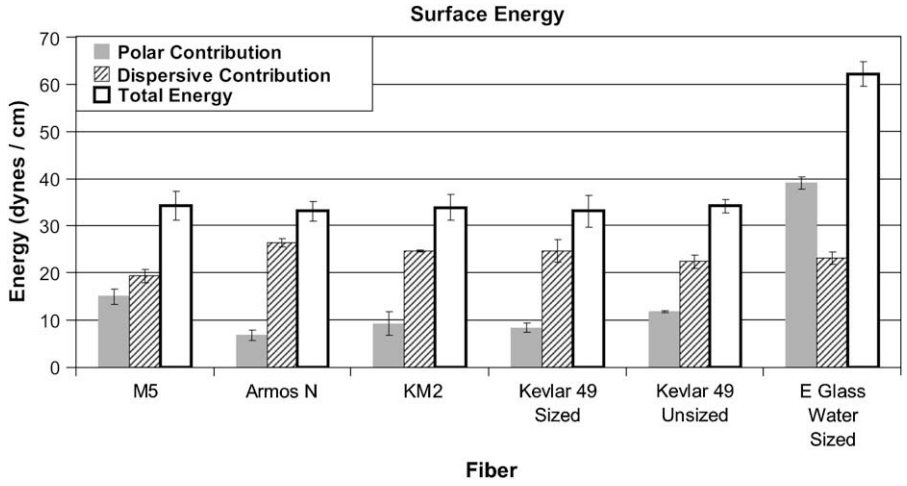

Fig. 5. Surface free energy of high performance fibers.

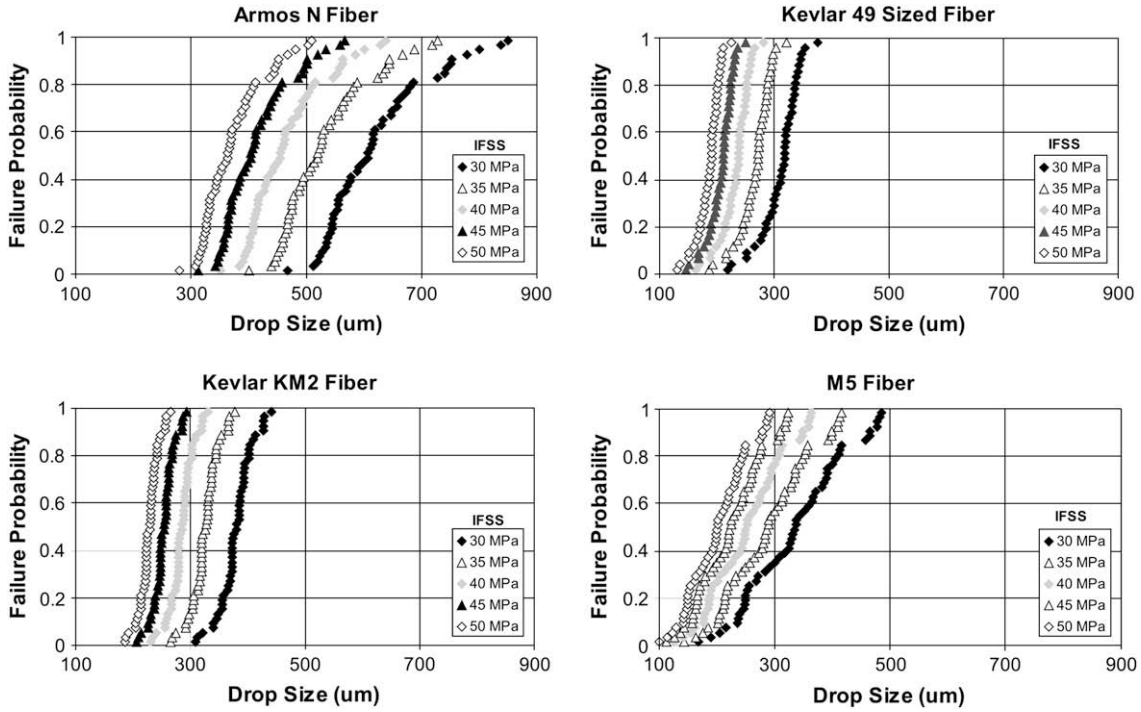

Fig. 6. Cumulative probability of fiber tensile failure during microdroplet testing as a function of droplet size (L).

$$L = \frac{\sigma^* d}{4^* \mathrm{IFSS}} \tag{4}$$

The cumulative probabilities of fiber tensile failure during microdroplet testing as a function of droplet size for different IFSS values are shown in Fig. 6 for Armos, Kevlar 49, Kevlar KM2 and M5 fibers. The probability of failure plots provide useful guidelines for microdroplet test specimen preparation.

Fig. 7 shows the IFSS of the different fibers under study, where the error bars represent ±one standard deviation. The figure indicates that M5 fiber has an average IFSS value that doubles that of the Kevlar fibers. This is in good agreement with previous results from surface free energy tests that show a higher polar contribution for M5 than the other organic fibers. The enhanced polar contribution, coupled with the presence of hydroxyl groups on the M5 surface that may react with an epoxide ring from the resin, yield a higher IFSS value. The large standard deviation observed in the case of M5 fiber could be associated to its experimental nature, which may lead to variations in the chemical nature of the fiber along its length. Given that a microdroplet specimen considers a very small section of the fiber, fluctuations in surface chemical nature could lead to an increased dispersion of the measured IFSS values [16,17]. Fig. 7 indicates that the Armos fibers have an average IFSS 30–35% higher than the Kevlar fibers. The more acidic Armos A fiber establishes slightly stronger interfacial bonds than the neutral Armos N fiber, in agreement with interfacial strength values reported by Kotomin et al. [18]. Although the increased IFSS of Armos with respect to the aramid fibers could be due in part to

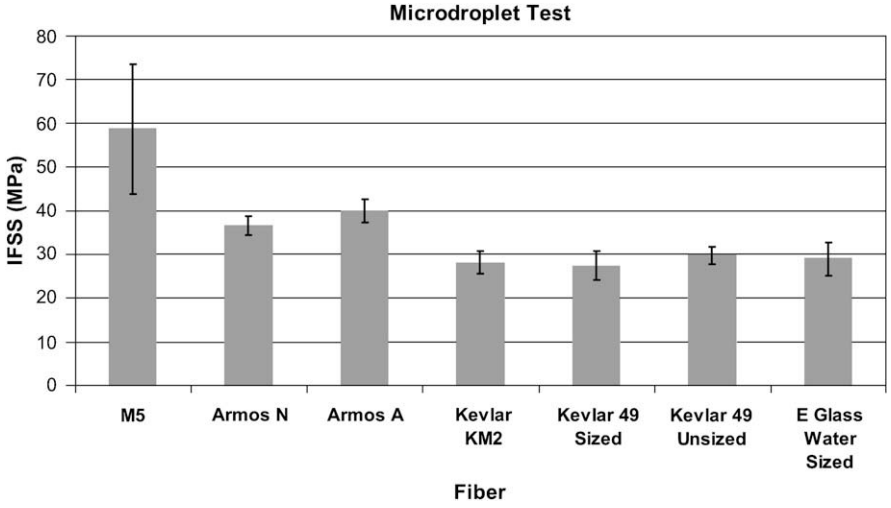

Fig. 7. Fiber interfacial shear strength.

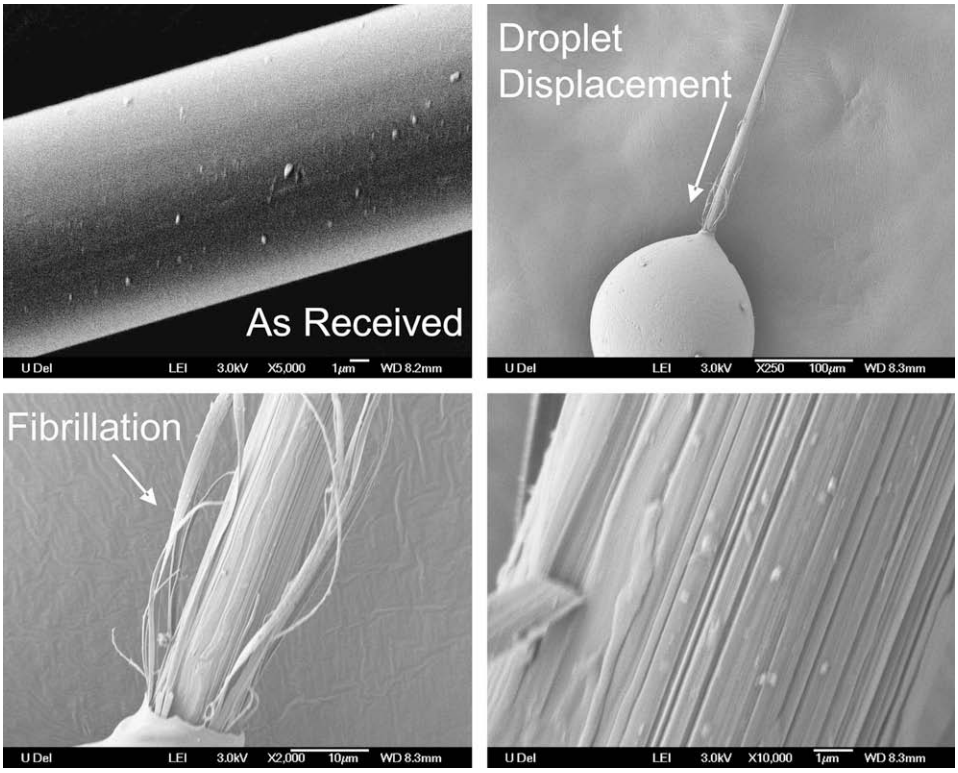

Fig. 8. SEM micrographs of failed Kevlar KM2 microdroplet specimens.

surface morphology characteristics that provide for larger mechanical interlocking between fiber and resin, chemical functionalities such as the imidazole group present in the heterocyclic component of the para-aramid Armos fiber may be establishing chemical interactions with the epoxy resin as well. The water-sized E-glass fiber shows a low IFSS value, comparable to the Kevlar fibers. However, it is important to note that the sizing chemistry for glass fibers is well developed, and that IFSS values in the order of

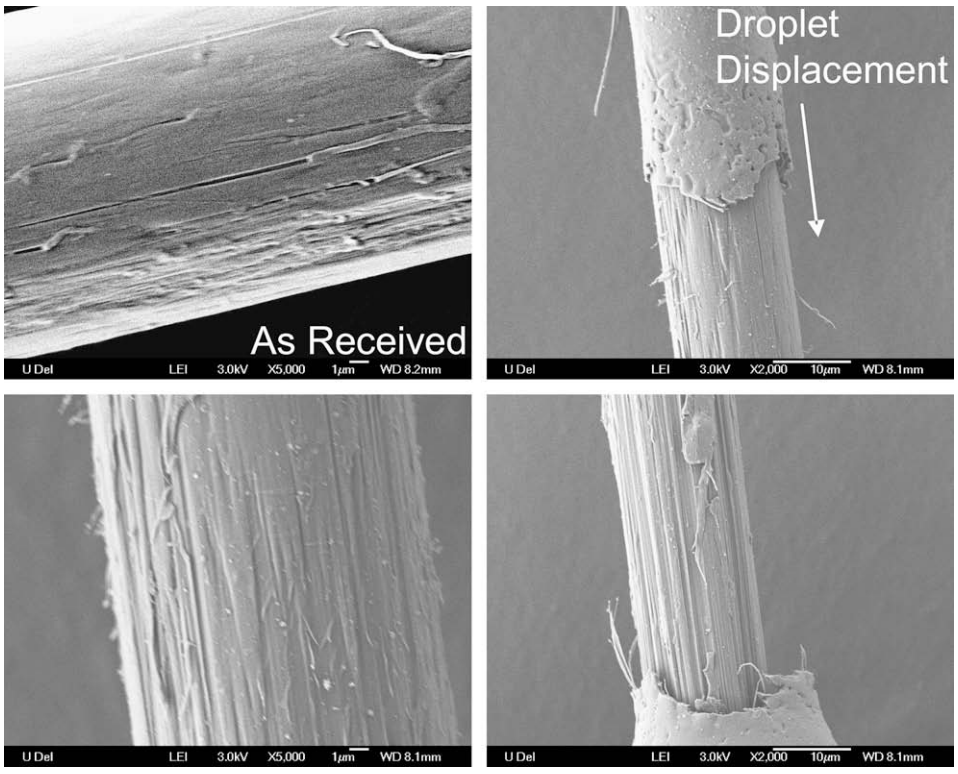

Fig. 9. SEM micrographs of failed Armos microdroplet specimen.

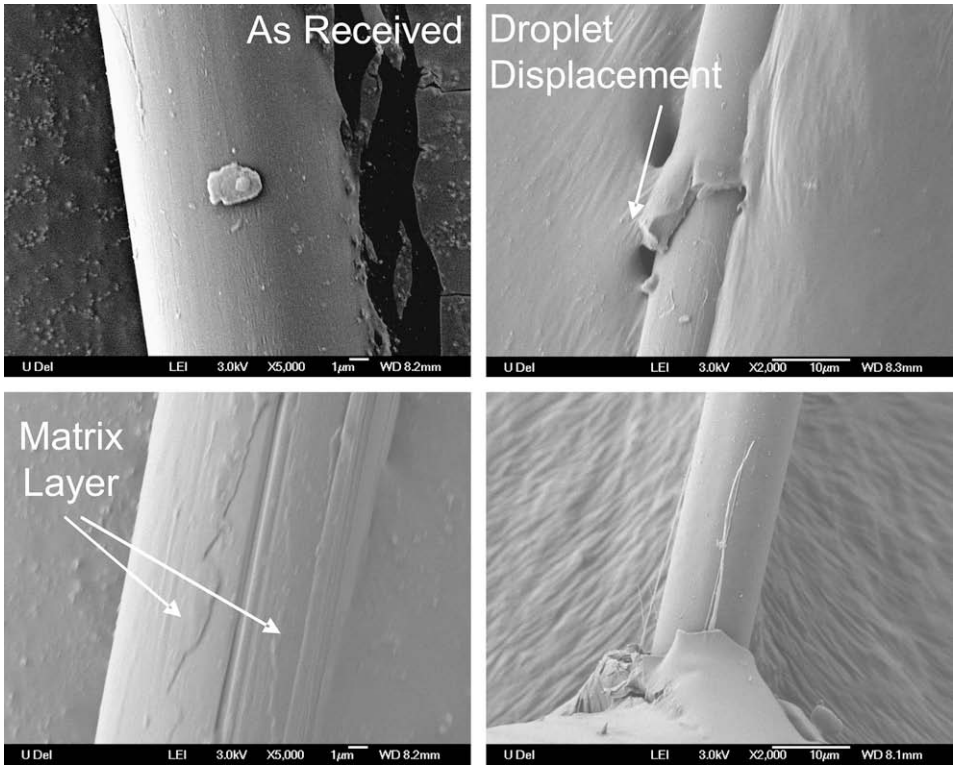

Fig. 10. SEM micrographs of failed M5 microdroplet specimen.

50 MPa have been achieved by means of functionalized sizings [19]. Use of a different epoxy resin to prepare the microdroplet specimens should not affect the observed trends of interfacial shear strength for the fibers included in the analysis.

The failure mechanisms of Kevlar KM2, Armos and M5 microdroplet specimens have been identified by scanning electron microscopy (SEM). Fig. 8 shows SEM images of a failed Kevlar KM2 microdroplet specimen along with an image of an as-received KM2 filament, for comparison. The as-received KM2 filament shows a very smooth surface, while the microdroplet specimens, having an average interfacial shear strength value of 28 MPa, show extensive fiber damage, with fibrils at the surface completely detached from the bulk of the fiber. This indicates that the shear strength between polymer chains in the fiber is weaker or at most only comparable to the interfacial shear strength between fiber and matrix. Failure of aramid–epoxy interfaces as a result of fibrillation at the fiber surface has also been observed by Kalantar and Drzal [20,21]. These results indicate that any effort to improve shear properties of systems using this fiber should concentrate on enhancing lateral interactions such as hydrogen bonding in the fiber before developing surface treatments to further improve the adhesion.

In the case of the Armos fiber microdroplet specimens shown in Fig. 9, it can be seen that the as-received Armos fiber has a higher degree of surface texture than Kevlar KM2, which may increase the IFSS value through mechanical interlocking. The SEM images of the failed Armos microdroplet specimens show some damage on the fiber surface, which looks rougher than the surface of the as-received fiber. The tested filament has maintained its cohesion, as opposed to what was observed for KM2, which is an indication of improved lateral interactions for Armos with respect to the KM2. In this case, the shear strength between microfibrils in the fiber seems to be comparable or slightly higher than the interfacial shear strength between fiber and resin. Failure in the Armos specimens is probably the result of detachment of microfibrils from the fiber surface coupled with adhesive failure. The fiber shows an interfacial shear strength value of 37 MPa, 30% higher than the value obtained for KM2.

The final microdroplet specimen failure mechanism to be discussed is observed in the M5 specimens. The as-received M5 filament shown in Fig. 10 has a fairly smooth surface. Looking at the microdroplet specimens, the fiber held together and its surface shows very little damage after droplet debonding. With $52 \pm 4\%$ of the amine groups in this fiber hydrogen-bonded intermolecularly to neighboring polymer chains [22], the shear strength between microfibrils in the fiber is definitely higher than the interfacial shear strength between fiber and matrix. This well-developed network of intermolecular hydrogen bonds is reported in the literature as the main reason for the significant improvements in compressive and shear properties of the fiber [11,23]. In addition, the SEM micrographs in Fig. 10 show what appears to be a layer of polymer matrix left behind on the fiber surface. The polar imidazole and hydroxyl functional groups on this fiber may be developing covalent bonds with the epoxide rings in the matrix, leading to partial matrix yielding during debonding. The average interfacial shear strength for the M5 specimens is 59 MPa, a value 2.1 times higher than the value obtained for the Kevlar KM2 specimens.

Given that M5 fiber is still at the development stage, it will be very interesting to monitor the progress of its interfacial and surface properties as the fiber reaches the commercial stage, while in the area of aramid fibers, it is important to ascertain the interfacial behavior of materials such as AuTX™-HT fiber.

4. Conclusions

Fiber total surface free energy calculations have shown that M5 fiber has a markedly higher polar contribution than the rest

of the organic fibers under consideration, which can lead to the formation of an interphase region at the M5 fiber surface with different mechanical properties from the bulk matrix. Analysis of the failure mechanisms induced by the microdroplet test indicates that Kevlar KM2, with an IFSS of 28 ± 3 MPa, has weak intermolecular fiber interactions that cause failure at low shear strength as a result of defibrillation. Armos fiber, with an IFSS 1.3 times higher than Kevlar KM2, fails during microdroplet testing due to the combined effect of microfibrillation and adhesive failure. In contrast, for M5 fiber specimens, with an IFSS 2.1 times higher than Kevlar KM2, failure during microdroplet testing is the result of partial matrix yielding during droplet debonding.

Acknowledgements

The authors wish to acknowledge the financial support provided by the Composite Materials Technology (CMT) Collaborative Program sponsored by the US Army Research Laboratory under Cooperative Agreement DAAD19-01-2-0005. Additionally, the authors would like to thank Dr. Philip Cunniff for providing the M5® fiber and Dr. Sergey Lopatnikov for his help in obtaining the Armos® fiber.

References

[1] Leal AA, Deitzel JM, Gillespie JW. Compos Sci Technol 2007;67:2786.
[2] Leal A, Deitzel J, Li W, Gillespie JW. In: Fiber Science-The Next Generation. The Fiber Society 2005 Fall Annual Meeting and Technical Conference: 17–19 October, New Jersey Institute of Technology, Newark, NJ, USA; 2005.
[3] Wang J, Chen P, Li H, Li W, Wang B, Zhang C, et al. Surf Interface Anal 2008; 40:1299.
[4] Wu GM. Mater Chem Phys 2004;85:81.
[5] Park JM, Kim DS, Kim SR. J Colloid Interface Sci 2003;264:431.
[6] Bedoui F, Murthy NS, Zimmermann FM. J Mater Sci 2008;43:5585.
[7] Herrera-Franco PJ, Drzal LT. Composites 1992;23:2.
[8] Andrews MC, Bannister DJ, Young RJ. J Mater Sci 1996;31:3893.
[9] Gaur U, Miller B. Compos Sci Technol 1989;34:35.
[10] Miller B, Muri P, Rebenfeld L. Compos Sci Technol 1987;28:17.
[11] Klop EA, Lammers M. Polymer 1998;39(24):5987.
[12] Levchenko AA, Antipov EM, Plate NA, Stamm M. Macromol Symp 1999;146:145.
[13] Kinloch AJ. Adhesion and adhesives. 1st ed. New York: Chapman and Hall; 1987 [chapter 2].
[14] Larson BK, Drzal LT. Composites 1994;25(7):711.
[15] Palmese GR. Ph.D. Dissertation, University of Delaware; 1992.
[16] Penn LS, Lee SM. J Compos Tech Res 1989;11:23.
[17] Penn LS, Tesoro GC, Zhou HX. Polym Compos 1988;9:184.
[18] Kotomin SV, Basharov VG, Bova VG, Sapozhnikov EM. Fibre Chem 1996;28(1):48.
[19] Gao X, Jensen RE, Li W, Deitzel J, McKnight SH, Gillespie JW. J Compos Mater 2008;42(5):513.
[20] Kalantar J, Drzal LT. J Mater Sci 1990;25:4186.
[21] Kalantar J, Drzal LT. J Mater Sci 1990;25:4194.
[22] Leal Ayala AA. Ph.D. Dissertation, University of Delaware; 2008.
[23] Hageman JCL, de Wijs GA, de Groot RA, Klop EA. Polymer 2005;46:9144.